

Large Attractive Depletion Interactions in Soft Repulsive–Sphere Binary Mixtures

Giorgio Cinacchi*

*Dipartimento di Chimica e Chim. Ind. , Università di Pisa,
Via Risorgimento 35, I-56126 Pisa, ITALY*

Yuri Martínez–Ratón

*Grupo Interdisciplinar de Sistemas Complejos (GISC), Departamento de Matemáticas,
Escuela Politécnica Superior, Universidad Carlos III de Madrid,
Avenida de la Universidad 30, E-28911 Leganés, Madrid, SPAIN*

Luis Mederos

*Instituto de Ciencia de Materiales de Madrid,
Consejo Superior de Investigaciones Científicas,
E-28049 Cantoblanco, Madrid, SPAIN*

Guillermo Navascués

*Departamento de Física Teórica de la Materia Condensada,
Universidad Autónoma de Madrid, E-28049 Madrid, SPAIN*

Alessandro Tani

*Dipartimento di Chimica e Chim. Ind., Università di Pisa,
Via Risorgimento 35, I-56126 Pisa, ITALY*

Enrique Velasco

*Departamento de Física Teórica de la Materia Condensada
and Instituto de Ciencia de Materiales Nicolás Cabrera,
Universidad Autónoma de Madrid, E-28049 Madrid, SPAIN*

Abstract

We consider binary mixtures of soft repulsive spherical particles and calculate the depletion interaction between two big spheres mediated by the fluid of small spheres, using different theoretical and simulation methods. The validity of the theoretical approach, a virial expansion in terms of the density of the small spheres, is checked against simulation results. Attention is given to the approach toward the hard-sphere limit, and to the effect of density and temperature on the strength of the depletion potential. Our results indicate, surprisingly, that even a modest degree of softness in the pair potential governing the direct interactions between the particles may lead to a significantly more attractive total effective potential for the big spheres than in the hard-sphere case. This might lead to significant differences in phase behavior, structure and dynamics of a binary mixture of soft repulsive spheres. In particular, a perturbative scheme is applied to predict the phase diagram of an effective system of big spheres interacting via depletion forces for a size ratio of small and big spheres of 0.2; this diagram includes the usual fluid-solid transition but, in the soft-sphere case, the metastable fluid-fluid transition, which is probably absent in hard-sphere mixtures, is close to being stable with respect to direct fluid-solid coexistence. From these results the interesting possibility arises that, for sufficiently soft repulsive particles, this phase transition could become stable. Possible implications for the phase behavior of real colloidal dispersions are discussed.

PACS numbers: 82.70.Dd

I. INTRODUCTION

Colloidal systems are complex fluids composed of mesoscopic particles dispersed in a solvent of microscopic particles. The large difference in size between the dispersed (colloidal) and the solvent entities may allow the latter to be considered as a continuum¹.

One way to prevent colloidal particles from aggregating is to sterically stabilize them, i.e. to coat them with a suitable polymer layer. This leads to an effective repulsive interaction, frequently considered so steep that colloidal particles have been extensively modeled as hard bodies. Thus, a dispersion made of spherical colloidal particles may in a first approximation be assimilated to a system of hard spheres (HS), the phase behavior of which is well known. In this respect, systems of mono-sized polymethylmethacrylate particles provide a good example².

The case of binary colloidal dispersions, where two colloidal species of different size are immersed in a molecular solvent, is less clear. Here the HS model may also be used to characterize colloidal interactions. Sophisticated integral-equation theories for binary HS fluid mixtures indicate that, contrary to the prediction of the Percus-Yevick closure³, demixing between two phases of different compositions may occur, provided the diameters of the two components are sufficiently different⁴. Binary mixtures of silica particles were shown to undergo phase-separation⁵, but its nature was not ascertained. The possibility that the phases involved were both fluid could not be excluded, but recent work has given evidence that demixing involves fluid and solid phases, and that fluid-fluid segregation in HS mixtures should be excluded^{6,7,8,9}.

The mechanism supposed to be at the basis of these demixing phenomena is known as the *depletion effect*, according to which there exists an effective *attractive* interaction between the big particles due to their clustering leading to a larger free volume available for the small particles. It was first put forward by Asakura and Oosawa¹⁰, and later reconsidered by Vrij¹¹, to explain the phase behavior of colloid-polymer mixtures. Depletion effects are invoked to explain a large variety of phenomena in mixtures and have been the subject of intense theoretical effort in recent years. The validity of the effective one-component approximation (big colloidal particles interacting via a depletion potential) in describing the phase behavior of the actual binary HS mixture has been checked by comparison of the phase behavior obtained from the effective potential of mean force using computer simulation, with

that obtained from direct computer simulations of the mixture^{7,8}. These studies revealed that fluid–fluid phase separation is actually unstable with respect to a fluid–solid phase transition; other computer simulation studies, based again on the effective one–component approach, showed no indication of any (even metastable) fluid–fluid demixing¹², suggesting that slightly different approximations for the depletion potential employed may lead to quite different phase behavior.

The very shape of the depletion potential appears to be very sensitive to small variations in the direct interactions among particles. For instance, slight degrees of non–additivity in binary HS systems result in depletion potentials which are very different from those calculated for the corresponding additive binary mixtures¹³. Also, residual interactions of short range and moderate strength, such as very short–ranged *attractive* Yukawa tails, which *prima facie* would appear irrelevant compared to the dominant hard–body terms, have been shown to significantly affect phase behavior¹⁴, tending to make the effective interactions *less* attractive. Moreover, the importance of carefully taking into account the colloidal–colloidal direct interactions has been stressed¹⁵: the total effective potential is the sum of the direct and indirect (depletion) contributions, and clearly the final shape depends on very fine details of both.

The above–mentioned sensitivity of (and on) the shape of the depletion potential undermines the rather common view that mixtures of sterically–stabilized spherical colloidal particles resemble HS mixtures, and serves as a stimulus for further investigations. In particular, a largely ignored, and probably more realistic, variation on the hard–sphere theme is to consider particles to have soft, rather than hard, repulsive cores. Although quite convincing experimental evidence exists about the fact that colloidal particles coated with poly–12–hydroxystearic acid, one of the most frequently used coating agents, should really behave as hard spheres in many solvents¹⁶, it appears of relevance to investigate depletion interactions in *repulsive* particles of various degrees of softness. In fact, the softness of the interaction potential was shown to have a pronounced influence on the crystal nucleation of model colloidal systems¹⁷, while interactions between colloidal particles may be tuned to a certain degree, for example by varying the chemical composition and thickness of the surface layer, to such an extent that soft–core colloidal particles can be realized¹⁸.

In this work, binary fluid mixtures of model soft repulsive spherical particles have been considered. The depletion interaction between two big particles induced by the small-particle

component has been evaluated using computer simulation. The depletion interaction can be obtained quite straightforwardly, using Molecular Dynamics (MD) simulation, as the potential of mean force on a big sphere. Systems of various densities have been analyzed and the results compared with various approximations based on a virial expansion. The most salient feature of the resulting depletion potential is that the effective attraction between soft spheres is greatly enhanced with respect to the HS case: as the softness is increased, the attraction becomes substantially larger, and the effective diameter of the big spheres is reduced. Since these trends of the interaction potential tend to promote fluid–fluid separation in liquids, the interesting possibility arises that fluid–fluid demixing could be stabilized in these fluids of repulsive particles. In an effort to explore this possibility, we have applied a perturbative scheme to evaluate the free energy, and from there the complete phase diagram, for a size ratio of small and big spheres of 0.2. These results already indicate that fluid–fluid demixing, which a related theoretical calculation predicts it to be absent in the case of HS mixtures, is close to being stable with respect to direct fluid–solid phase separation, suggesting that further variations of the interactions, for example by further softening the interaction potentials, might induce the stability of a liquid phase in mixtures of soft repulsive spheres.

The article is organized as follows. In Sec. II interaction models, simulation techniques and theoretical approximations for the depletion potential are described. Results are contained in Sec. III, and the conclusions are presented in Sec. V.

II. THEORETICAL APPROACH AND SIMULATION DETAILS

The fluids considered in this work are binary mixtures whose constituents are spherical particles of two species, i and j , interacting by a pair potential $u_{ij}(r)$ defined as

$$u_{ij}(r) = \begin{cases} 4\epsilon_{ij} \left[\left(\frac{\sigma_{ij}}{r} \right)^{2n} - \left(\frac{\sigma_{ij}}{r} \right)^n + \frac{1}{4} \right], & r \leq 2^{1/n} \sigma_{ij}, \\ 0, & r > 2^{1/n} \sigma_{ij}, \end{cases} \quad (1)$$

with ϵ_{ij} and σ_{ij} the energy and range parameters, respectively, and r the distance between the two interacting particles. n , henceforth called ‘softness parameter’, is an exponent such that the limit $n \rightarrow \infty$ gives the HS case. The rate at which the HS limit is approached

as $n \rightarrow \infty$ in $u_{ij}(r)$ is dictated by the temperature T . As n is decreased from this limit the repulsive potential becomes softer. For the case $n = 6$ this potential corresponds to the repulsive part of the Weeks–Chandler–Andersen separation scheme for the Lennard–Jones potential¹⁹. In this work, $\epsilon_{ij} = \epsilon \forall i, j$, while the size parameters for the two species have been given the following values: $\sigma_{11} = \sigma$, $\sigma_{22} = 0.2\sigma$, $\sigma_{12} = \sigma_{21} = 0.6\sigma$ (here an additivity rule is applied on the σ_{ij} parameters; in this way the limit $n \rightarrow \infty$ exactly corresponds to additive hard spheres). Particles of the species labeled as 1 will therefore be referred to as big, solute or colloidal spheres, while particles labeled as 2 will be called small or solvent spheres.

One can define a total interaction potential $U(r)$ between two isolated big spheres immersed in the fluid of small spheres. This potential will have two contributions: the direct, or bare, contribution, given by $u_{11}(r)$, and an indirect contribution, $W(r)$, which is transmitted through the small spheres and is actually the potential of mean force; this contribution is identified as the depletion potential, and the total potential will be calculated as $U(r) = u_{11}(r) + W(r)$. One of the aims of this work is to study how the depletion interaction, and consequently the total effective interaction between the two big particles varies not only with the density of the solvent, ρ_2 , but also with the degree of softness, n , and the temperature T .

In the case of generic particle systems, it is convenient to measure physical quantities in reduced units. Thus, we will define reduced densities as $\rho_i^* = \rho_i \sigma_{ii}^3$, $i = 1, 2$, while a reduced temperature will be given as $T^* = k_B T / \epsilon = (\beta \epsilon)^{-1}$, with $\beta = 1/k_B T$ and k_B Boltzmann’s constant.

1. *Virial expansion for the depletion potential*

The density functional formalism has been successfully applied to calculate the depletion potential in HS mixtures^{20,21}. Due to the lack of density functionals of proven adequacy for soft–sphere systems²², we need to implement an alternative approach. One possibility is a systematic approach that provides a perturbative expansion for the depletion potential in powers of the solvent density. In the following we discuss such an expansion, which has been discussed before and applied to HS mixtures^{9,12}.

Within the second–order virial approximation, the grand potential associated to the solvent particles, interacting via a pair potential $u_{22}(r)$ and in the external potential $u_{12}(r)$

corresponding to a colloidal particle located at the origin, is

$$\begin{aligned} \beta\Omega[\rho_2] &= \int d\mathbf{r} \rho_2(\mathbf{r}) [\ln \rho_2(\mathbf{r}) - 1] + \frac{1}{2} \int d\mathbf{r} \int d\mathbf{r}' \rho_2(\mathbf{r}) \rho_2(\mathbf{r}') f_{22}(\mathbf{r} - \mathbf{r}') \\ &+ \beta \int d\mathbf{r} [u_{12}(\mathbf{r}) - \mu_2] \rho_2(\mathbf{r}), \end{aligned} \quad (2)$$

where $\rho_2(\mathbf{r})$ is the density distribution of the solvent particles. $f_{ij} = 1 - \exp(-\beta u_{ij})$ is the Mayer function associated with the interaction between particles of species i and j (note that here it is defined with a negative sign with respect to the standard definition). Within the same approximation, the chemical potential μ_2 corresponding to a reservoir of solvent particles with constant density ρ_2 is given by

$$\beta\mu_2 = \ln \rho_2 + \rho_2 \int d\mathbf{r}' f_{22}(\mathbf{r} - \mathbf{r}'). \quad (3)$$

Functional minimization of Eqn. (2) with respect to $\rho_2(\mathbf{r})$ and use of Eqn. (3) gives the following integral equation for the equilibrium density profile $\rho_2(\mathbf{r})$:

$$\rho_2(\mathbf{r}) = \rho_2 \exp \left[-\beta u_{12}(\mathbf{r}) - \int d\mathbf{r}' [\rho_2(\mathbf{r}') - \rho_2] f_{22}(\mathbf{r} - \mathbf{r}') \right]. \quad (4)$$

We will obtain the solution to Eqn. (4) perturbatively, i.e. assuming the validity of the density expansion

$$\rho_2(\mathbf{r}) = \rho_2 \Psi_1(\mathbf{r}) + \rho_2^2 \Psi_2(\mathbf{r}) + \dots. \quad (5)$$

The functions $\Psi_i(\mathbf{r})$ are found by inserting Eqn. (5) into Eqn. (4); at first and second order in ρ_2 we find

$$\Psi_1(\mathbf{r}) = \exp[-\beta u_{12}(\mathbf{r})], \quad (6)$$

$$\Psi_2(\mathbf{r}) = \exp[-\beta u_{12}(\mathbf{r})] \int d\mathbf{r}' f_{12}(\mathbf{r}') f_{22}(\mathbf{r} - \mathbf{r}'). \quad (7)$$

Up to third order in density, the contribution to the virial expansion of the excess part of the free-energy functional of the binary mixture containing terms linear in $\rho_1(\mathbf{r})$ is

$$\begin{aligned} \beta\mathcal{F}_{\text{ex}}^{(1)}[\rho_1, \rho_2] &= \int d\mathbf{r} \int d\mathbf{r}' \rho_1(\mathbf{r}) \rho_2(\mathbf{r}') f_{12}(\mathbf{r} - \mathbf{r}') \\ &+ \frac{1}{2} \int d\mathbf{r} \int d\mathbf{r}' \int d\mathbf{r}'' \rho_1(\mathbf{r}) \rho_2(\mathbf{r}') \rho_2(\mathbf{r}'') f_{12}(\mathbf{r} - \mathbf{r}') f_{12}(\mathbf{r} - \mathbf{r}'') f_{22}(\mathbf{r}' - \mathbf{r}''). \end{aligned} \quad (8)$$

Using the definition of $c_1^{(1)}(\mathbf{r}; [\rho_1, \rho_2])$, the one-body direct correlation function for big spheres, i.e. $c_1^{(1)}(\mathbf{r}; [\rho_1, \rho_2]) = -\delta\beta\mathcal{F}_{\text{ex}}[\rho_1, \rho_2]/\delta\rho_1(\mathbf{r})$, we find the dilute limit $\rho_1 \rightarrow 0$ from

Eqn. (8) as

$$\begin{aligned}
-c_1^{(1)}(\mathbf{r}; [\rho_1 = 0; \rho_2]) &= \int d\mathbf{r}' \rho_2(\mathbf{r}') f_{12}(\mathbf{r} - \mathbf{r}') \\
&+ \frac{1}{2} \int d\mathbf{r}' \int d\mathbf{r}'' \rho_2(\mathbf{r}') \rho_2(\mathbf{r}'') f_{12}(\mathbf{r} - \mathbf{r}') f_{12}(\mathbf{r} - \mathbf{r}'') f_{22}(\mathbf{r}' - \mathbf{r}'').
\end{aligned} \tag{9}$$

The limit $\rho_1 = 0$ represents the infinite dilution limit of the mixture with respect to the big spheres. As shown in Ref.^{20,21}, the depletion potential between two big particles in the sea of solvent particles can be obtained from

$$\beta W(\mathbf{r}) = c_1^{(1)}(\infty; [\rho_1 = 0, \rho_2]) - c_1^{(1)}(\mathbf{r}; [\rho_1 = 0, \rho_2]). \tag{10}$$

Note that the calculation of the pair depletion potential requires the evaluation of the functional $c_1^{(1)}(\mathbf{r}; [\rho_1 = 0, \rho_2])$ at the equilibrium density profile of small particles in the presence of only one big sphere, $\rho_2(\mathbf{r})$, whose effect is taken care of by an external potential. This feature makes density functional theory to be a powerful tool to calculate solvation forces in multicomponent mixtures^{20,21}.

Substituting Eqn. (9) into Eqn. (10) and using Eqn. (5), with the expressions found for $\Psi_i(\mathbf{r})$, Eqns. (6) and (7), we arrive finally at

$$W(\mathbf{r}) = W^{(\text{AO})}(\mathbf{r}) + W^{(\text{B3})}(\mathbf{r}), \tag{11}$$

$$\beta W^{(\text{AO})}(\mathbf{r}) = -\rho_2 \int d\mathbf{r}' f_{12}(\mathbf{r}') f_{12}(\mathbf{r} - \mathbf{r}'), \tag{12}$$

$$\beta W^{(\text{B3})}(\mathbf{r}) = \rho_2^2 \int d\mathbf{r}' \int d\mathbf{r}'' f_{12}(\mathbf{r} - \mathbf{r}') f_{22}(\mathbf{r}' - \mathbf{r}'') \mathcal{K}(\mathbf{r}, \mathbf{r}', \mathbf{r}''), \tag{13}$$

where the kernel

$$\mathcal{K}(\mathbf{r}, \mathbf{r}', \mathbf{r}'') = e^{-\beta u_{12}(\mathbf{r}')} f_{12}(\mathbf{r}'') + \frac{1}{2} \left\{ e^{-\beta [u_{12}(\mathbf{r}') + u_{12}(\mathbf{r}'')] } - 1 \right\} f_{12}(\mathbf{r} - \mathbf{r}'') \tag{14}$$

has been defined. The Asakura-Oosawa (AO) approximation given by Eqn. (12), and the more accurate approximation given by Eqns. (11)–(14), which also includes a contribution from three-body interactions [see Eqn. (8)] will be checked against computer simulations in Sec. III. All integrals involved in Eqns. (12) and (13) have been evaluated numerically using Gaussian quadratures. The above procedure can be systematically continued to obtain higher-order contributions to the depletion potential. However, inclusion of the next term, proportional to $(\rho_2)^3$, requires the evaluation of multidimensional integrals with a numerical

cost comparable to that required in MD simulations of the exact depletion potential. This is the reason why we stop the density expansion at second order in the present work.

Let us now examine the predictions of the above two approximations with respect to density ρ_2^* and softness parameter n . Fig. 1 shows, for values of the softness parameter $n=6, 12$ and ∞ , the depletion potential $W(r)$ evaluated with the AO approximation, Eqn. (12), at a density $\rho_2^* = 0.0409$, sufficiently low that the use of this approximation could in principle be justified, and at a temperature $T^*=0.776$. The figure includes plots of the direct interaction $u_{11}(r)$ between two bigger particles, as well as the resulting total interaction potential, $U(r) = u_{11}(r) + W(r)$, obtained by the sum of direct and indirect contributions. Significant differences can be seen among the attractive depletion interactions as the softness parameter is changed: in particular, the softer the pair interactions, the longer-ranged the attractive contribution. As expected, the depletion potential in the case of the hard sphere binary mixture vanishes at a distance $r^* \equiv r/\sigma = 1.2$, while $W(r)$ in the case of soft spheres does so at progressively larger distances. All depletion potentials follow the same trend, but the softest direct potential, corresponding to the case $n = 6$, exhibits a more attractive indirect interaction. This effect is partly counterbalanced by the fact that in this case the direct interaction potential is softer, remaining positive at larger distances than in the other cases (in fact, direct interactions vanish at a distance $r^* = 2^{1/n}$, which increases as n is reduced); the net effect is that the energy minimum U_{\min} of the total interaction potential deepens and shifts to shorter distances as n is increased. Now, a convenient measure of the well width is given by the quantity $w_n = (r_2^{(n)} - r_1^{(n)})/r_1^{(n)}$, with $r_i^{(n)}$ being the distance between the origin and the i th root of $U(r)$. Using this criterion, it can be seen that the potential well becomes wider as the direct interactions operating in the mixture become softer. All these trends, which occur at the level of the AO approximation, are monotonic with the degree of softness.

This situation changes to a certain extent when corrections from the second-order density terms are incorporated, as illustrated in Fig. 2. Here depletion potentials are calculated by employing Eqns. (11)–(14) at densities $\rho_2^* = 0.2045$ [Fig.2(a)] and $\rho_2^* = 0.4090$ [Fig. 2(b)], both at $T^*=0.776$. As expected, the depletion potentials become more negative with density. In addition, they start to show maxima at distances $r^* \sim 1.15$ – 1.20 ; these maxima become more pronounced as density is increased. The existence of an associated repulsive barrier in the depletion potentials is a well-established fact, first shown in Ref.²⁴. The height of

the maximum is rather insensitive to n , while its location decreases very slightly with n . However, by looking jointly at Fig. 1 and 2, the combined action of ρ_2^* and n is noticeable. For relatively low values of ρ_2^* , the smallest value of U_{\min} is observed for $n \rightarrow \infty$, while U_{\min} is a monotonically decreasing function of n . In the same density regime, the width of the potential energy well, w_n , decreases steadily with ρ_2^* at a fixed value of n ; the same monotonically decreasing behavior of w_n with n occurs even at higher densities, so that $w_6 > w_{12} > w_\infty$ always. However, contrary to w_∞ , which persists in decreasing with density, w_{12} at $\rho_2^* = 0.4090$ is almost the same as that at $\rho_2^* = 0.2045$, whereas w_6 at the higher density is even larger than the value at $\rho_2^* = 0.04090$. Finally, the value of U_{\min} for finite n approaches that for $n \rightarrow \infty$, still the most negative, but in a nonmonotonic way, as the value of U_{\min} for $n = 6$ is larger than that for $n=12$.

Summing up to this point, we have shown that the density expansion of the depletion potential up to second order indicates that the predictions of the simple AO approximation, namely that the potential well associated to the total interaction shifts to longer distances and becomes less attractive with respect to the hard-sphere case as the direct interactions become softer, are different at higher fluid densities: the potential well and its depth behave nonmonotonically with the softness parameter. A full calculation, valid to all orders in density, is needed to elucidate whether these trends could give rise to enhanced attractive interactions with respect to the hard-sphere mixture when the interactions become sufficiently soft.

2. Details on MD simulations

The predictions presented in the previous section are based on a density expansion of $W(r)$. Since it is not practical to improve our approximation beyond the second order in density, one has to resort to computer simulation in order to check the validity of the results of the last section. We have carried out extensive MD simulations on a system of two big spheres immersed in a fluid of small spheres, calculating the depletion potential directly; this technique allows us to obtain depletion potentials which are, in principle, exact at all densities.

In the above theoretical derivation, it has been assumed from the beginning that the two big spheres remained fixed at certain positions and that their effect on the small spheres

could be taken into account by means of an external potential. In our MD simulations, two methods have been used to freeze the dynamics of the big spheres.

In the first method, the distance, r , between the big spheres has been maintained fixed in the course of the simulation run by using the method of constraints reviewed in Ref.²⁵. Note that we assume the two spheres to form a dimer, with translational and rotational degrees of freedom; it is only the dynamics associated to the relative distance between the two big spheres which is frozen. This introduces an additional contribution to the free energy per particle with respect to the case where the centers of mass of the two big spheres are fixed, coming from the volume and solid angle explored by the dimer, but averaged quantities such as the potential of mean force are not affected. In the second method we fix the centers of mass of the big spheres, which therefore act as an external potential on the small spheres. In both methods, the force, $F(r)$, acting on these bigger particles due to the smaller particles, has been calculated according to the formula first used in Ref.²⁶ to evaluate the potential of mean force between two ions in a polar solvent, and already applied in the context of colloid physics in Ref.²⁷, that is:

$$F(r) = \frac{1}{2} \left\langle \hat{\mathbf{r}} \cdot \sum_{j=1}^{N_2} \left(\mathbf{F}_j^{(a)} - \mathbf{F}_j^{(b)} \right) \right\rangle \quad (15)$$

In the above equation $\hat{\mathbf{r}}$ is the unit vector defining the direction of the vector joining the two big spheres, a and b , while $\mathbf{F}_j^{(i)}$ is the force on the big sphere $i = a, b$ due to the small sphere j . The angular brackets indicate an average over the configurations of the small particles generated during the simulation run. This method cannot be applied in HS mixtures, which require evaluation of the surface density distribution on the big spheres; possible inaccuracies introduced by extrapolation to contact of the density histogram obtained from the simulation are not present here. Statistical errors are of the same order, however, since in both, HS- and soft-sphere mixtures, the fluctuating quantity is averaged over $O(N_2)$ values.

Systems of two big particles, each of mass m_1 , immersed in a sea of $N_2=2046$ or 4000 small particles (depending on the method used to calculate the depletion force), each one of mass $m_2 = m_1$, have been simulated with standard MD simulation techniques. Periodic boundary conditions are applied on the rectangular simulation box. The simulations have been carried out for the cases $n=6$ and 12, integrating the equation of motion with the Verlet algorithm²⁸, using a time step of $5 \times 10^{-4} \tau$, τ being equal to $\sigma_{11}(m_1/\epsilon)^{1/2}$, and maintaining the temperature at the desired value via the Nosé-Hoover thermostat²⁸. For each finite

value of n investigated, several distances have been considered, at which the depletion force is calculated during production runs of $1-3 \times 10^5$ time steps, preceded by 5×10^4 time steps of equilibration. The depletion potential is then obtained by numerically integrating this force. Before integration, forces have been smoothed out by fitting to an appropriate function or by Akima spline approximation²⁹. The integration constant has been set so that the depletion potential was chosen to be zero at the largest radial distance considered.

The solvent density, ρ_2^* , which should correspond to the density of the reservoir of solvent particles, is evaluated by computing the time-averaged density profile at the boundaries, i.e. far from the big spheres, averaging over the boundaries to suppress fluctuations. This density does not exactly coincide with that obtained by dividing N_2 by the volume available to the small spheres, since the density profile is highly structured in the region next to the big spheres.

Using the techniques described above, depletion interaction potentials, $W(r)$, and their corresponding total effective potentials, $U(r)$, have been calculated for a few values of the density ρ_2^* , the softness parameter n and the temperature T^* .

III. PRESENTATION AND DISCUSSION OF THE RESULTS

In this section we check the depletion potential resulting from the density expansion proposed above, see Eqns. (11)–(14), against our simulation results. The purpose of this exercise is to elucidate whether a truncated density expansion is adequate to describe depletion effects; in particular, we would like to estimate the maximum solvent density for which the truncated expansion is quantitatively valid. Then, the behavior of the depletion potentials obtained from simulation with respect to density, softness parameter and temperature will be assessed.

A. Check of virial expansion against computer simulation

First we compare the predictions obtained from the truncated virial expansion for a fixed softness parameter, $n = 6$, with the simulations results, at fixed temperature $T^*=1.000$ and for several values of ρ_2^* . Fig. 3 shows the results of this comparison. It appears that the first-order expansion, corresponding to the AO theory, insufficiently accounts for the simulation

data even at the lowest density considered, $\rho_2^* = 0.190$. The incorporation of the next term in the density expansion improves significantly the performance of the theory with respect to simulation. The agreement between the outcome of Eqn. (11) and the simulation data is very good for $\rho_2^* = 0.190$ at all distances. Increasing the density, the agreement naturally deteriorates but is still quite fair at $\rho_2^* = 0.381$ for distances $0.80 < r^* < 1.15$. In contrast, the agreement between theory and simulation is poor at the very high density $\rho_2^* = 0.740$, which indicates that higher-than-second order terms should be included in the density expansion.

Due to the “compensatory” effect of the addition of the direct interaction potential $u_{11}(r)$ at the shortest distances, the agreement between the second-order virial expansion theory and simulation is better if the total effective potentials are examined (Fig. 4). For $\rho_2^* = 0.190$, Eqn. (11) predicts a potential $U(r)$ which is almost indistinguishable from that of simulation. At $\rho_2^* = 0.381$, the agreement between the two curves is still fairly good, especially with regard to the location and width of the attractive well, while the subsequent tiny maximum is displaced and its height slightly overestimated. It is only at larger values of the density of the smaller spherical particles, such as $\rho_2^* = 0.565$, that the two potentials show noticeable discrepancies. For $\rho_2^* = 0.740$, the results disagree considerably even in the attractive region.

By confronting Eqns. (12) and (11–14) together, and by exploiting the results just presented, one can conclude that Asakura–Oosawa theory can be used to construct accurate total effective potentials up to density $\rho_2^* \simeq 0.05$; the inclusion of the quadratic term is necessary for densities in the range $0.05 \lesssim \rho_2^* \lesssim 0.40$, while for larger densities at least the cubic term is to be used. Once we have assessed the density range where the virial expansion is valid, we now turn to explore the dependence of the depletion and total effective potentials obtained from simulation with respect to density, the degree of softness and the temperature.

B. Dependence of the depletion potential on density, n and temperature

Fig. 5 shows the values of the depletion force, calculated from MD simulation, as a function of distance, for two values of the softness parameter, $n = 6$ and $n = 12$, and for two high densities, $\rho_2^* = 0.680$ and $\rho_2^* = 0.750$; the temperature is $T^* = 0.776$. Note that the values of density chosen are certainly below the freezing density of the WCA fluid, which accurate estimations based on computer simulation locate at $\rho_2^* \simeq 0.91$ for $T^* = 1.0$ ³⁰. In

all cases the depletion force has been evaluated in the region of small distances as well; note that $F(r)$ vanishes at $r = 0$, i.e. when the two big spheres are exactly superimposed, because of symmetry. The computations of the depletion potential at such small distances could appear *prima facie* useless, as the direct interactions are so largely dominant in these conditions that the value of $W(r)$ does not affect that of $U(r)$. In particular, for hard-body systems, the evaluation of depletion forces at distances shorter than the contact distance is clearly useless in the construction of the effective pair potential. Indeed, previous simulation studies on hard-sphere binary mixtures have only reported data at distances larger than the contact distance^{31,32}, and theoretical efforts have tried to reproduce these data (*e.g.* Ref.^{20,21}). Nonetheless, indirect interactions are clearly defined for all distances, regardless of the nature of the direct interactions, and their evaluation at very small distances should be of importance *per se* as they constitute a set of numerical data against which theories should be tested.

The shapes of the depletion forces shown in Fig. 5 are clearly consistent with two distinct regimes as the radial distance r is changed: a shallow and deep minimum at scaled distances smaller than unity, and an oscillating part at longer distances. The value of the minimum is rather insensitive to the degree of softness but depends strongly on the value of density, while the location of the minimum is weakly n -dependent. Changing these two parameters gives rise to rather different oscillatory structures, the amplitude and damping of the latter being larger for increasing values of density and softness parameter.

As shown in Fig. 5, the depletion forces have been fitted, using empirical functions which reflect the existence of these two regimes²⁹. The depletion potentials have been then obtained by integrating the corresponding fitting function. The results are shown in Fig. 6, which contains the direct interaction potentials together with the resulting total effective pair potentials $U(r)$. Unfortunately, simulation data on the analogous hard-sphere binary systems are available only up to a density of $\rho_2^* = 0.74$ ³². Thus, in order to make a comparison, the parametrized formula derived in Ref.²¹ for the depletion potential in hard-sphere mixtures has been used at the highest density considered, $\rho_2^* = 0.750$. From that figure, one can see that for the two densities considered, $\rho_2^* = 0.680$ and 0.750 , not only the well width but also the depth of the total effective interactions between the big soft spheres are larger than in the hard-sphere case, and in the case of the softest potential, $n = 6$, the attractive interactions are considerably enhanced.

This result concurs with those of Ref.¹⁵ about the importance of taking into account the direct interaction between the big particles. The total effective interactions which govern the thermodynamical, structural and dynamical properties of these particle systems, is in fact the sum of two contributions which may have, as in the present case, different signs but comparable absolute values in an interval of distances close to the range of the interaction between the big spheres. Thus, the final shape of the total effective pair potential is clearly very sensitive to the details of the direct and indirect contributions, both on the same footing.

However, in contrast with the results in Ref.¹⁴, where attractive interactions were considered and depletion interactions of varying nature (attractive or even repulsive) were obtained, in the case of repulsive direct interactions the depletion potentials are always attractive and, at high fluid densities, greatly enhanced with respect to those obtained for HS mixtures. In the light of these results, and considering that in some cases HS mixtures exhibit a metastable fluid–fluid phase separation, one may wonder whether enhanced attractive depletion forces may change the nature of demixing phenomena in mixtures. This topic will be discussed in the next section.

One last issue in the present subsection involves the dependence of the depletion potential on temperature, a dependence that certainly exists as the model particles interact via smooth, as opposed to hard, interactions. Therefore, the total interaction potential will in general be a parametric function not only of density, but also of temperature, $U(r; \rho_2^*, T^*)$. Fig. 7 shows the MD–derived depletion and total effective potentials obtained for $n=6$ at densities $\rho_2^* = 0.381$ and 0.740 , and temperatures $T^* = 0.776$ and 1.000 . As expected, density has a larger, dominant effect. Differences between the two depletion potentials corresponding to the same density but different temperatures are discernible only at the shortest distances, the two functions being essentially superimposed for $r^* > 1$. In the case $\rho_2^* = 0.381$ the total interaction potentials are very close even at short distances, where the two functions are positive. When $\rho_2^*=0.740$ the difference is larger at these distances, but still small. Irrespective of the value of density, the depletion potential becomes stronger as temperature is increased, which is reflected in the total effective potential having a deeper and wider attractive well; this can be understood in view of the higher momentum interchanged between particles at higher temperatures, which involves larger kinetic pressures (and hence larger depletion effects) and more penetrable spheres. In this respect, although density can be considered in the present context as the more physically interesting variable,

being responsible for the largest variations in the effective potentials, the modest effect of temperature seen in Fig. 7 could have a large impact on the phase behavior and properties of binary mixtures of the type investigated in this work.

IV. CALCULATION OF THE PHASE DIAGRAM FOR THE REPULSIVE SOFT-SPHERE MIXTURE WITH $n=6$

In the previous sections we have presented results for the depletion potentials of mixtures of soft spheres at various densities of the small spheres. These potentials have been computed, either using the virial expansion or by computer simulation, under the assumption of infinite dilution of the big spheres. Invoking the two-body approximation, we may assume that this is the potential felt by any two pairs of big spheres when their density is arbitrarily large. Indeed, the effect of three-particle interactions on the depletion potential has been argued to be overall very small^{31,33,34,35}. In addition, we have made our own estimates of this effect by computing the force on a trimer of big soft spheres, in an equilateral triangular configuration, at a distance between the spheres $r = \sigma_{11} + \sigma_{22}$, which approximately coincides with the maximum of the depletion potential, and then subtracting the pair force associated to the three bonds; the remainder is the three-body contribution. Our calculation indicates that this contribution can be neglected altogether, confirming previous expectations^{31,33,34,35} in hard-sphere mixtures.

We now consider a collection of big spheres at density ρ_1^* interacting via the depletion potential calculated at a density of small spheres ρ_2^* . As mentioned in the introduction, a longstanding discussion was whether or not a similar mixture of hard spheres exhibits demixing, i.e. a first-order phase transition where two phases with different concentration of big and small spheres coexist. The current understanding is that hard-sphere mixtures do exhibit demixing, but it involves a fluid phase and a crystalline phase, or two crystalline phases⁷. Since, as we have shown, soft repulsive spheres are influenced by a much stronger depletion force than in the case of hard spheres, it is pertinent to ask the following questions: (i) Does a mixture of soft-repulsive spheres exhibit demixing? (ii) Is the tendency toward segregation stronger than in the hard-sphere case? (iii) Does demixing involve two fluid phases, rather than one or the two being crystalline? Since we only intend to explore the possible phase behaviors of the mixture, we have applied a perturbation theory to calculate

the phase diagram; an alternative, in principle exact computer simulation approach is for the moment ruled out because of its relatively high computational cost. The theory is a density–functional theory based on the weighted–density approximation where a perturbation term is added, the so–called perturbative weighted density approximation (PWDA). The perturbative term is evaluated using the compressibility equation to fine–tune the effective radial distribution function in the crystal phase. This procedure involves a mapping onto an effective HS fluid. Even though the theory cannot be trusted for liquid densities beyond the crystallisation density for hard spheres, for densities less than that the predictions of the theory should be qualitatively correct. More details on the theoretical procedure can be found in Ref.³⁶.

The resulting phase diagram, in the $\rho_1^*-\rho_2^*$ plane, is shown in Fig. 8. The continuous lines correspond to the fluid–solid binodal lines obtained from the PWDA theory using depletion potentials calculated from the second–order virial expansion, Eqn. (11). The dashed lines are the corresponding calculation of the spinodal lines for fluid–fluid phase separation; note that the low-density spinodal should be given qualitatively correctly by the PWDA theory (maybe not so in the case of the high–density spinodal). It can be seen that fluid–fluid separation is always metastable with respect to the fluid–solid transition. PWDA calculations based on depletion potentials calculated from simulation are indicated by symbols. As expected, the two results are very similar for low values of ρ_2^* , where the truncated virial expansion is supposed to be accurate. At higher densities ρ_2^* , the two sets of depletion potentials give different but compatible results (for both binodal and spinodal lines).

For the sake of illustration we include in Fig. 8, as dotted lines, the results for the fluid–solid binodal line from a slightly different version of perturbation theory³⁷ as applied to the corresponding HS mixture using the depletion potential of Roth et al.²¹. In fact, the HS fluid–fluid spinodal line predicted by this theory occurs at very high solvent densities, too high to appear in the range of Fig. 8; given that the effective depletion potential is not valid in this regime²¹, we conclude that, for the present value of size ratio, fluid–fluid phase separation in effective HS mixtures is, if anything, highly metastable with respect to direct fluid–solid phase equilibrium. In contrast, in the case of soft interactions, fluid–fluid phase separation is close to being stable with respect to fluid–solid phase separation. The predictions of perturbation theory as to the large differences between HS and soft–

sphere mixtures is very significant and illustrate the effect on the phase behavior of the significantly more attractive effective interactions operating in soft-sphere mixtures than in the corresponding HS mixtures.

One can speculate on possible variations of the soft repulsive bare potentials (in the direction of making them even softer, for instance) that could promote the stability of the fluid phase, and its associated critical point, with respect to the solid phase. Actually, recent work^{38,39} supports the possibility that an increasingly deeper and, especially, wider attractive well could lead to the observation of a stable fluid–fluid phase separation in these binary systems. In any case, use of an improved theory and more extensive simulations on fluids with other types of interactions and at different temperatures are needed, since the final outcome appears to be the result of a delicate free-energy balance between the fluid and the solid. Further exploration of these topics are left for future work.

V. CONCLUDING REMARKS

The present results are considered pertinent to real experimental binary colloidal dispersions. It is known that many of them exhibit a fluid–fluid demixing transition and a phase behavior which is temperature dependent (for a discussion of the effect of temperature on the properties of sterically stabilized colloidal systems see Ref.⁴⁰), two facts that are not captured by assimilating the colloidal particles to hard bodies but that could be by modeling them as soft–core objects.

Indeed, the pair–potential models investigated should be relevant to sterically stabilized colloids. In these systems, the degree of softness of the direct interactions can be controlled by varying the chemical composition and/or, especially, the thickness of the coating polymer layer: we could in principle expect that an increase in thickness produces softer interactions. Recently, an experimental study has been carried out on binary dispersions formed by colloids sterically stabilized with a coating polymer layer of varying chemical composition and thickness¹⁸. Although no stable fluid–fluid separation was observed, evidence for weakly metastable fluid–fluid demixing has been suggested for the mixture with the thickest stabilizing layer. These results have been interpreted in terms of a non–additive hard–sphere model. However, another, perhaps physically more sound, explanation of these experimental facts can be given in terms of the degree of interaction softness. An interesting sequel of

the study of Hennequin et al.¹⁸ could be an investigation of additional binary suspensions of sterically stabilized colloids with varying thicknesses of the coating polymer layer. Further theoretical work along the lines presented in the previous section could also be valuable and guide possible experimental research avenues.

We hope that the present results will stimulate the search for real colloidal binary mixtures where interparticle interactions can be tuned from hard- to soft-sphere-like, as well as an investigation of how the phase behavior and the properties of such mixtures evolve upon changing such characteristics. Indeed, charge- and sterically stabilized monodisperse colloidal suspensions have recently been reported where the softness of the interactions is controlled by the concentration of the added salt⁴¹. Although the pair potential models investigated in this work are not appropriate for charge-stabilized colloids, as the presence of charges requires a different functional form for the model pair interactions, the observed evolution of the depletion and total effective interactions with density and degree of softness of the direct interactions should be quite general. Thus, we believe it would be interesting to extend the study of Ref.⁴¹ to bidisperse suspensions.

Acknowledgments

MIUR (Italy) and Ministerio de Educación y Ciencia (Spain) are thanked for financial support under the 2005 binational integrated program. Y.M.-R. was supported by a Ramón y Cajal research contract. This work is part of the research projects PRIN "Energy and Charge Transfers at molecular level" of MIUR (Italy), MOSAICO, FIS2005-05243-C02-01 and FIS2004-05035-C03-02 of the Ministerio de Educación y Ciencia (Spain), and S-0505/ESP-0299 of Comunidad Autónoma de Madrid (Spain).

* Electronic address: g.cinacchi@sns.it; URL: <http://www.dcci.unipi.it/~ivo/cinacchi.htm>

¹ W. B. Russell, D. A. Saville, W. R. Schonwalter, *Colloidal Dispersions*, Cambridge University Press, Cambridge (1992); R. J. Hunter, *Foundations of Colloid Science*, Oxford University Press, Oxford (2001).

² P. N. Pusey, W. Van Megen, *Nature* **320**, 340 (1986).

³ J. L. Lebowitz, J. S. Rowlinson, *J. Chem. Phys.* **41**, 133 (1964).

- ⁴ T. Biben, J. P. Hansen, *Phys. Rev. Lett.* **66**, 2215 (1991); T. Biben, J. P. Hansen, *J. Phys. Cond. Matt.* **3**, F65 (1991).
- ⁵ J. S. Van Duijneveldt, A. W. Heinen, H. N. W. Lekkerkerker, *Europhys. Lett.* **21**, 369 (1993).
- ⁶ H. N. W. Lekkerkerker and A. Stroobants, *Physica A* **195**, 387 (1993).
- ⁷ M. Dijkstra, R. Van Roij, R. Evans, *Phys. Rev. Lett.* **81**, 2268(1998).
- ⁸ M. Dijkstra, R. Van Roij, R. Evans, *Phys. Rev. Lett.* **82**, 117 (1999).
- ⁹ M. Dijkstra, R. Van Roij, R. Evans, *Phys. Rev. E* **59**, 5744 (1999).
- ¹⁰ S. Asakura, F. Oosawa, *J. Chem. Phys.* **22**, 1255 (1954); S. Asakura, F. Oosawa, *J. Polym. Sci.* **33**, 183 (1958).
- ¹¹ A. Vrij, *Pure Appl. Chem.* **48**, 471 (1976).
- ¹² N. G. Almarza, E. Enciso, *Phys. Rev. E* **59**, 4426 (1999).
- ¹³ R. Roth, R. Evans, A. A. Louis, *Phys. Rev. E* **64**, 051202 (2001).
- ¹⁴ P. Germain, J. G. Malherbe, S. Amokrane, *Phys. Rev. E* **70**, 041409 (2004).
- ¹⁵ P. Germain, M. Bouaskarne, J. G. Malherbe, C. Regnaut, S. Amokrane, *Prog. Colloid Polym. Sci.* **126**, 102 (2004).
- ¹⁶ G. Bryant, S. R. Williams, L. Qian, I. K. Snook, E. Perez, F. Pincet, *Phys. Rev. E* **66**, 060501(R) (2002).
- ¹⁷ S. Auer, D. Frenkel, *Adv. Polym. Sci.* **173**, 149 (2005).
- ¹⁸ Y. Hennequin, M. Pollard, J. S. Van Duijneveldt, *J. Chem. Phys.* **120**, 1097 (2004).
- ¹⁹ J. D. Weeks, D. Chandler, H. C. Andersen, *J. Chem. Phys.* **54**, 5237 (1971).
- ²⁰ B. Götzelmann, R. Roth, S. Dietrich, M. Dijkstra, R. Evans *Europhys. Lett.* **44**, 398 (1999).
- ²¹ R. Roth, R. Evans, S. Dietrich, *Phys. Rev. E* **62**, 5360 (2000).
- ²² One interesting, but in the present context yet untested, possibility could be the density functional theory developed in Ref.²³.
- ²³ M. Schmidt, *Phys. Rev. E* **62**, 3799 (2000).
- ²⁴ J. Y. Walz, A. Sharma, *J. Colloid. Interface Sci.* **168**, 485 (1994).
- ²⁵ G. Ciccotti, J. P. Ryckaert, *Comp. Phys. Rep.* **4**, 345 (1986).
- ²⁶ G. Ciccotti, M. Ferrario, J. T. Hynes, R. Kapral, *Chem. Phys.* **129** 241 (1989).
- ²⁷ H. Shinto, M. Myiahara, K. Higoshitani, *J. Colloid. Interf. Sci.* **209**, 79 (1999).
- ²⁸ M. P. Allen, D. J. Tildesley, *Computer Simulation of Liquids*, Oxford University Press, Oxford (1989).

²⁹ The shape of the depletion force suggests to fit the numerical data displayed in Fig. 5 with the following empirical function:

$$F^{\text{fit}}(r) = A [1 - f(\alpha r^\nu)] (r^\beta + ar) - bf(\alpha r^\nu) e^{-\kappa r} \cos [2\pi\delta (r - r_0)]$$

with $\{A, \alpha, \nu, \beta, a, b, \kappa, \delta, r_0\}$ the set of fitting parameters. Clearly this equation does not have any ambition to be a proper description of the functional dependence of depletion forces upon distance; it has just been used to smooth the numerical data. In the equation one can recognize two regimes: the attractive well described by the term $r^\beta + ar$, and the subsequent oscillatory damped part described by the exponential–sinusoidal term. The factor $f(\alpha r^\nu)$ and its complement to unity have the role of switching continuously from one regime to the other. The above functional form has proven to be quite effective for $n=6$, and not so much for $n=12$ (see Fig. 15); actually, for the computation of the potential $W(r)$ by integrating the force, the Akima spline method was used instead.

- ³⁰ S. Hess, M. Kröger and H. Voigt, *Physica A* **250**, 58 (1998).
- ³¹ T. Biben, P. Bladon, D. Frenkel, *J. Phys. Cond. Matt.* **8**, 10799 (1996).
- ³² R. Dickmann, P. Attard, V. Simonian, *J. Chem. Phys.* **107**, 205 (1997).
- ³³ S. Melchionna, J.P. Hansen, *Phys. Chem. Chem. Phys.* **2**, 3465 (2000).
- ³⁴ D. Goulding, S. Melchionna, *Phys. Rev. E* **64**, 011403 (2001).
- ³⁵ D. Zhu, W. Li, H.R. Ma, *J. Phys. Cond. Matt.* **15**, 8281 (2003).
- ³⁶ L. Mederos, G. Navascués, P. Tarazona and E. Chacón, *Phys. Rev. E* **47**, 4284 (1993); L. Mederos, G. Navascués and P. Tarazona, *Phys. Rev. E* **49**, 2161 (1994).
- ³⁷ E. Velasco, G. Navascués and L. Mederos, *Phys. Rev. E* **60** 3158 (1999).
- ³⁸ C. F. Tejero, A. Daanoun, H. N. W. Lekkerkerker, M. Baus, *Phys. Rev. Lett.* **73**, 752 (1994).
- ³⁹ M. Hasegawa, K. Ohno *J. Phys. Cond. Matt.* **9**, 3361 (1997); M. Hasegawa, *J. Chem. Phys.* **108**, 208 (1998).
- ⁴⁰ M. Silbert, E. Canessa, M. J. Grimson, O. H. Scalise, *J. Phys. Cond. Matt.* **11**, 10119 (1999).
- ⁴¹ A. Yethiraj, A. van Blaaderen, *Nature* **421**, 513 (2003).

FIGURE CAPTIONS

Figure 1: Dashed lines: depletion potentials calculated with Eqn. (12) for $n = 6$, $n = 12$ and $n \rightarrow \infty$ (from bottom to top). Dotted lines: direct potential for $n = 6$ (upper curve) and $n = 12$ (lower curve); the case $n \rightarrow \infty$ is a vertical line at $r = \sigma$. Continuous thick lines: from right to left, total effective potentials for $n = 6$, $n = 12$ and $n \rightarrow \infty$. All calculations for a density $\rho_2^* = 0.0409$ and temperature $T^* = 0.776$.

Figure 2: Dashed lines: depletion potentials calculated with Eqns. (11)–(14) for $n = 6$, $n = 12$ and $n \rightarrow \infty$. Dotted lines: direct potential for $n = 6$ (light gray) and $n = 12$ (gray); the case $n \rightarrow \infty$ is a vertical line at $r = \sigma$. Continuous thick lines: total effective potentials, corresponding to softness parameters $n = 6, 12$ and ∞ indicated by labels and different gray intensity. (a) $\rho_2^* = 0.2045$ and (b) $\rho_2^* = 0.4090$. In both cases $T^* = 0.776$.

Figure 3: Depletion potential for $n=6$ calculated using Eqn. (12) (dotted lines), Eqns. (11)–(14) (dashed lines), and MD simulations (solid lines) at densities $\rho_2^* = 0.190$ (a), 0.381 (b) and 0.740 (c). In all cases $T^* = 1.000$.

Figure 4: Total effective potentials for $n=6$ calculated using Eqns. (11)–(14) (dashed lines) and MD simulations (solid lines) at densities $\rho_2^* = 0.190$ (a), 0.381 (b), 0.565 (c) and 0.740 (d). In all cases $T^* = 1.000$.

Figure 5: The depletion force as a function of distance for: $n=6$, $\rho_2^* = 0.680$ (a); $n=6$, $\rho_2^* = 0.750$ (b); $n=12$, $\rho_2^* = 0.680$ (c); $n=12$, $\rho_2^* = 0.750$ (d). Dots are the simulation results while lines are fitting curves²⁹. In all cases $T^* = 0.776$. Insets are zooms of the regions about the maxima.

Figure 6: Dashed lines: depletion potentials obtained by integrating the depletion force calculated in the simulations for $n = 6$ and 12 (value of n indicated as a label). Dotted lines: direct potentials for $n = 6$ and 12 (the case $n = 6$ corresponds to the softer potential). Solid

lines: total effective potentials for $n = 6, 12$ and ∞ (HS), indicated by labels and different gray intensities (light, medium and dark, respectively). Results in (a) are for $\rho_2^* = 0.680$, while those in (b) are for $\rho_2^* = 0.750$. Data for HS mixtures ($n = \infty$) from simulations of Ref.³² (a), and from density functional theory of Ref.²¹ (b). Insets are enlargements of the regions about the maxima.

Figure 7: Effect of temperature on depletion (squares) and total effective (circles) interactions between two big spherical particles: (a) $\rho_2^*=0.381$; (b) $\rho_2^*=0.740$. Open symbols correspond to $T^* = 0.776$, while filled circles were calculated with $T^* = 1.000$. All results are for $n=6$.

Figure 8: Phase diagram for the effective one-component system in the plane $\rho_1^*-\rho_2^*$. Solid lines: fluid–solid binodal lines, as predicted by PWDA theory using virial approximation for depletion potential, Eqns. (11)–(14); dashed lines: fluid–fluid spinodal lines as obtained from the same theory. Dotted lines: fluid–solid binodals for a hard–sphere mixture of the same size ratio, as obtained from perturbation theory (see Ref.³⁷). Filled circles: fluid–solid phase boundaries as obtained from PWDA theory using depletion potential calculated from simulation. Open circles: fluid–fluid spinodal from the same theory. Filled squares: fluid–solid coexistence densities for the one–component WCA system from computer simulation (see Ref.³⁰). The value of the reduced temperature is $T^* = 1.000$.

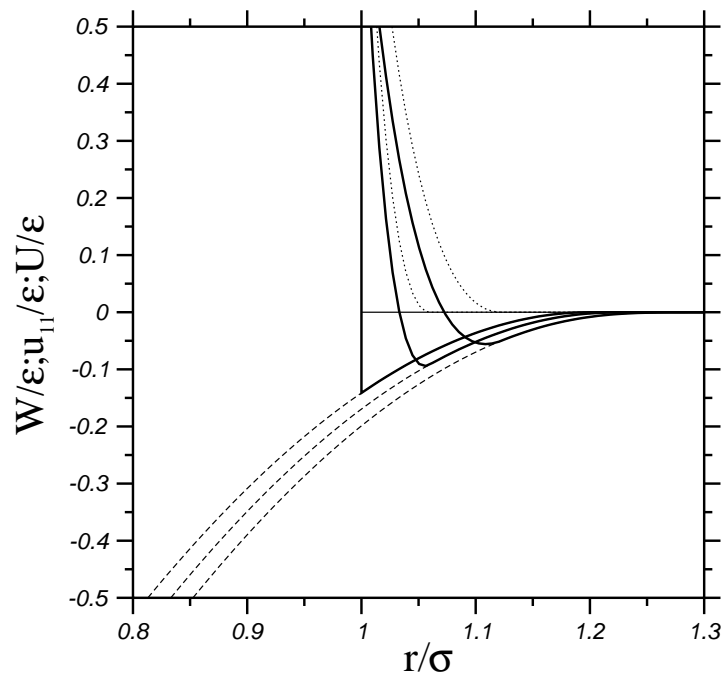


FIG. 1:

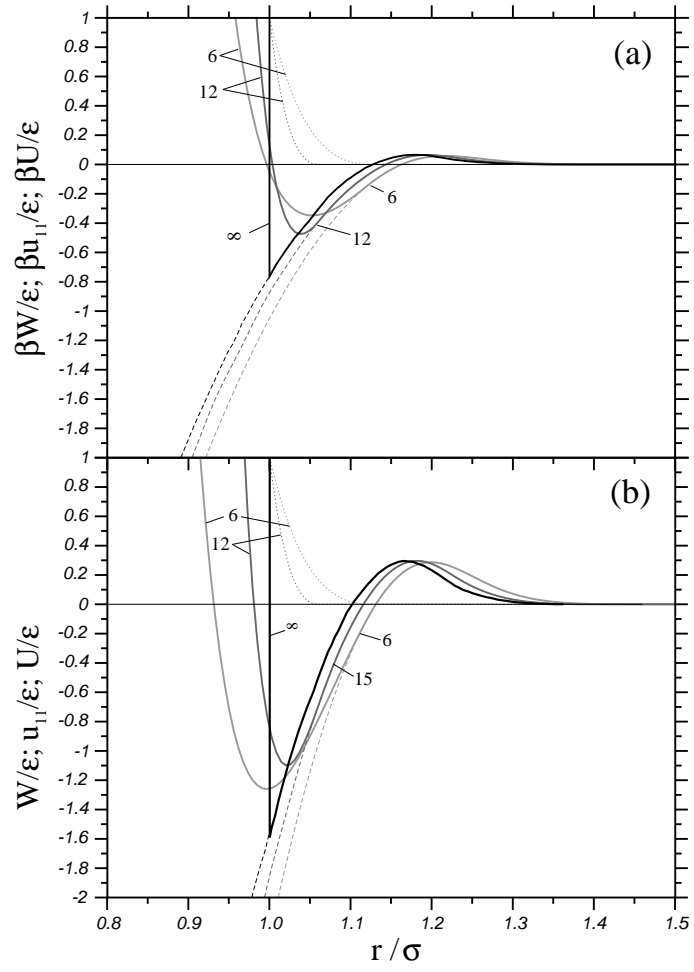


FIG. 2:

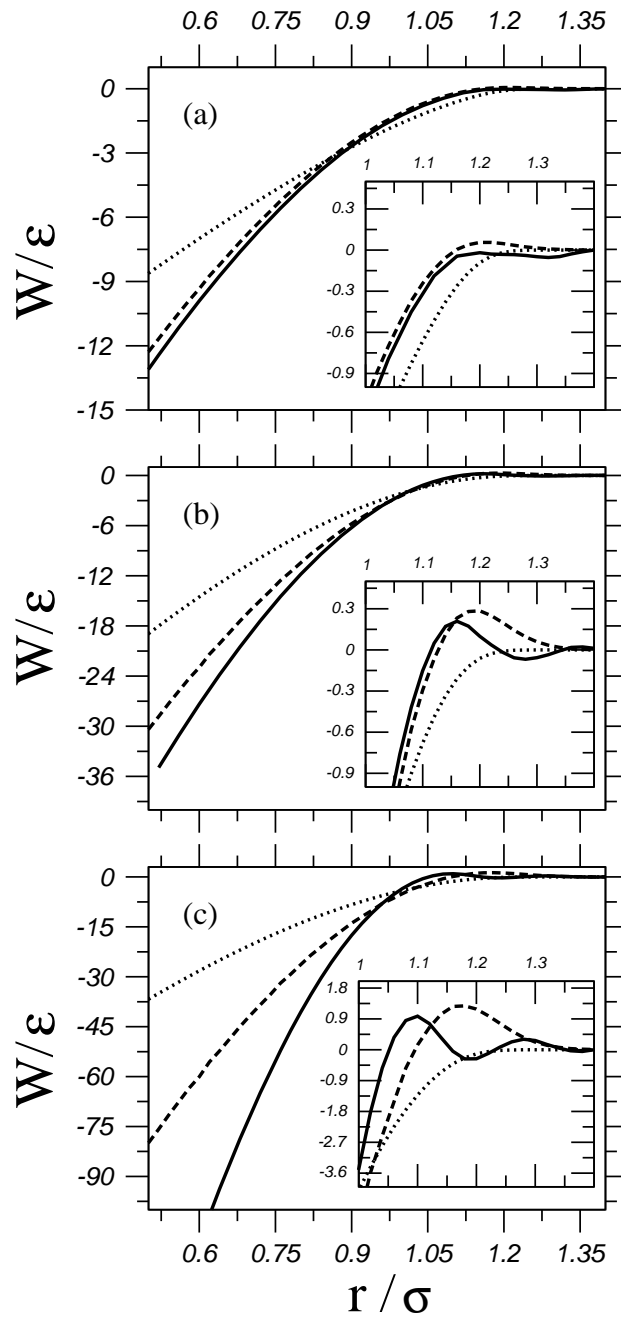


FIG. 3:

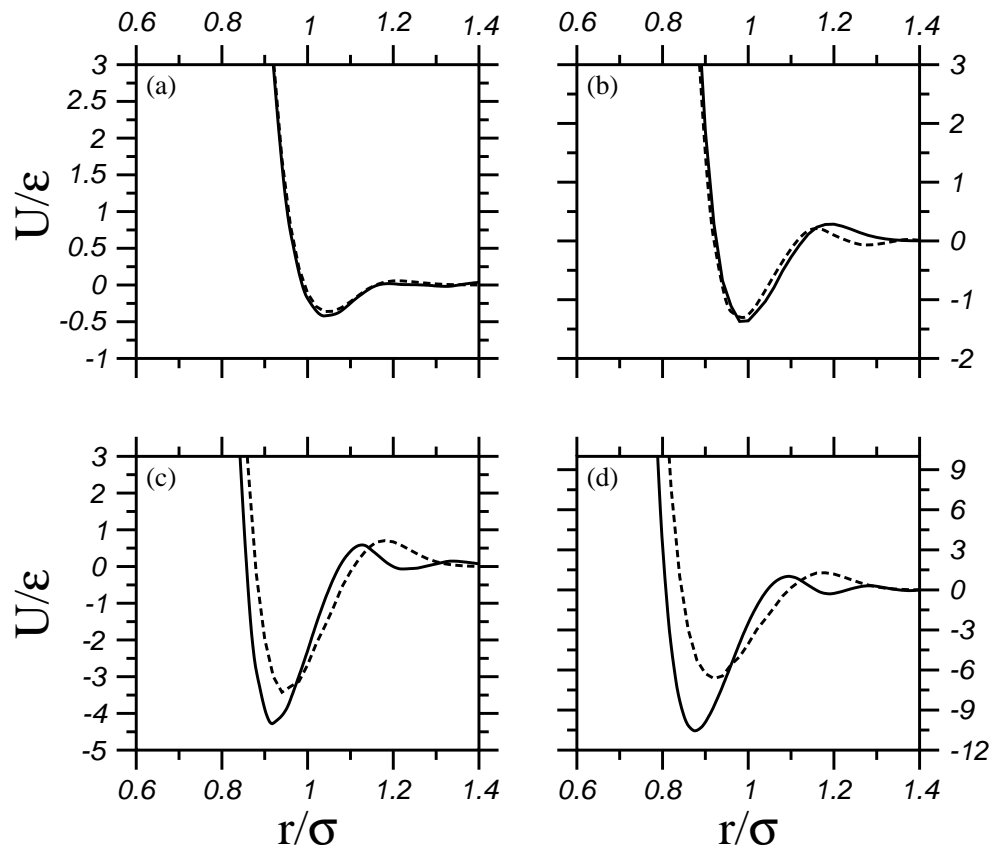


FIG. 4:

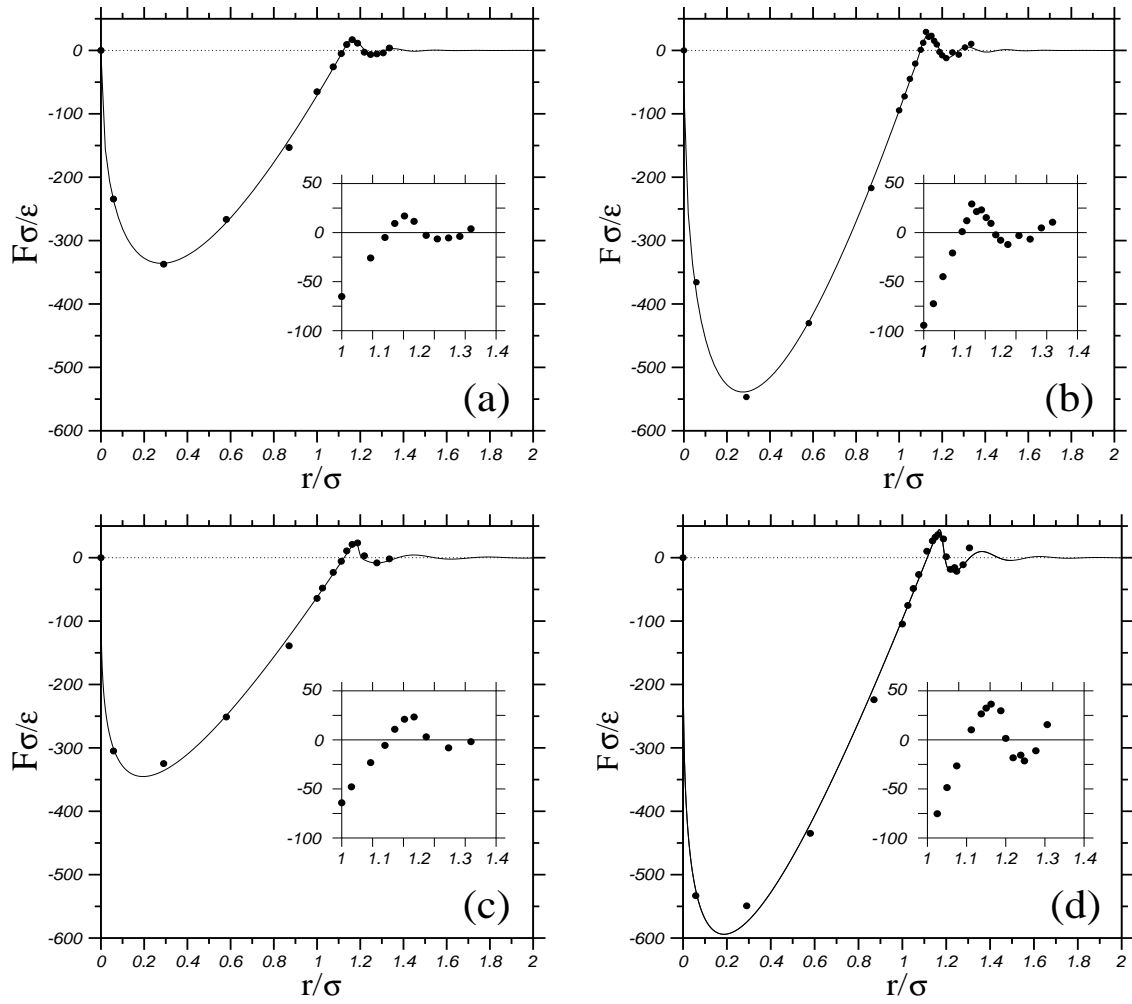


FIG. 5:

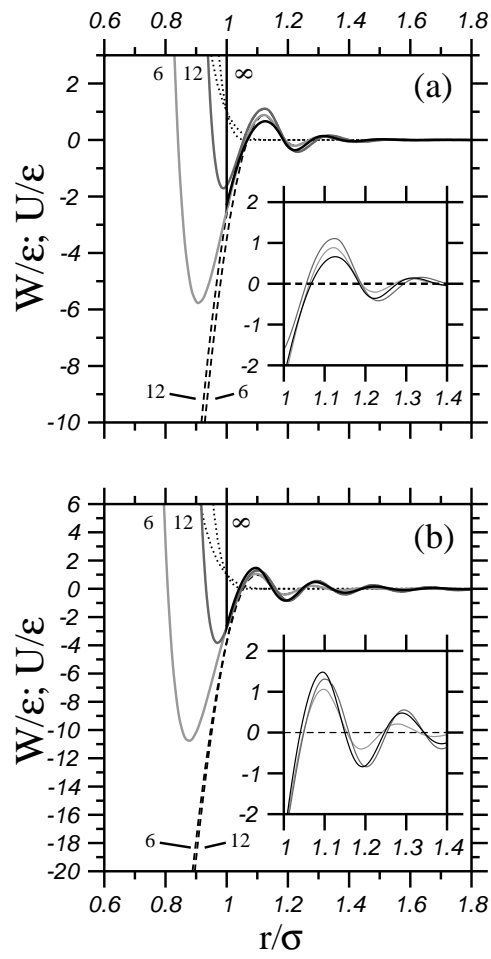


FIG. 6:

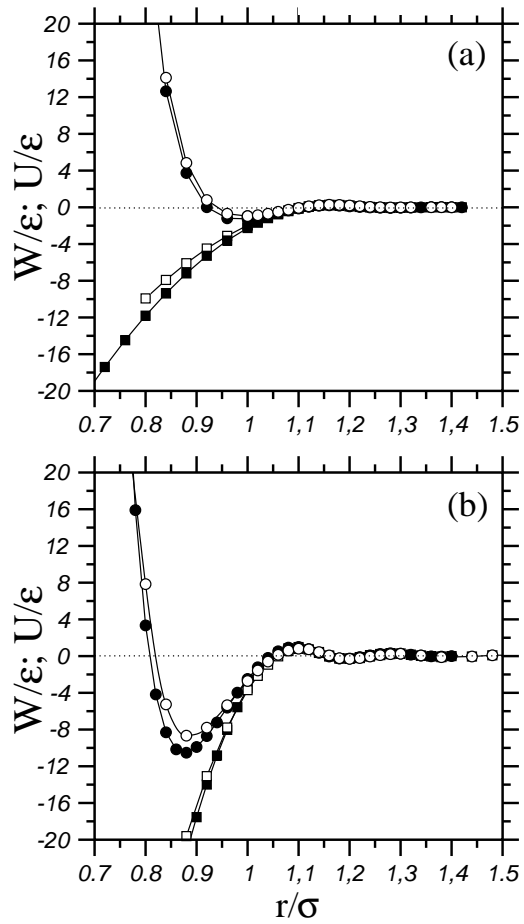


FIG. 7:

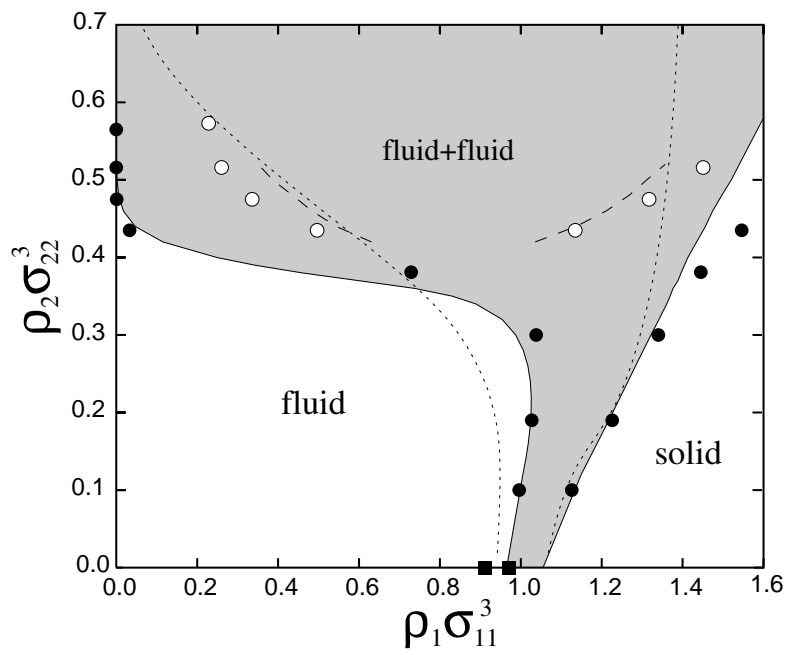


FIG. 8: